Novel Constraints on Axions Produced in Pulsar Polar-Cap Cascades

Dion Noordhuis [1,*,†] Anirudh Prabhu [2,3,†] Samuel J. Witte [1,†] Alexander Y. Chen,[4]
Fábio Cruz [5,6] and Christoph Weniger [1]

[1]*GRAPPA Institute, Institute for Theoretical Physics Amsterdam and Delta Institute for Theoretical Physics,
University of Amsterdam, Science Park 904, 1098 XH Amsterdam, Netherlands*
[2]*Princeton Center for Theoretical Science, Princeton University, Princeton, New Jersey 08544, USA*
[3]*Stanford Institute for Theoretical Physics, Stanford University, Stanford, California 94305, USA*
[4]*Physics Department and McDonnell Center for the Space Sciences, Washington University, St. Louis, Missouri 63130, USA*
[5]*GoLP/Instituto de Plasmas e Fusão Nuclear, Instituto Superior Técnico, Universidade de Lisboa, 1049-001 Lisboa, Portugal*
[6]*Inductiva Research Labs, Rua da Prata 80, 1100-420 Lisboa, Portugal*

Axions can be copiously produced in localized regions of neutron star magnetospheres where the ambient plasma is unable to efficiently screen the induced electric field. As these axions stream away from the neutron star they can resonantly transition into photons, generating a large broadband contribution to the neutron star's intrinsic radio flux. In this Letter, we develop a comprehensive end-to-end framework to model this process from the initial production of axions to the final detection of radio photons, and derive constraints on the axion-photon coupling, $g_{a\gamma\gamma}$, using observations of 27 nearby pulsars. We study the modeling uncertainty in the sourced axion spectrum by comparing predictions from 2.5 dimensional particle-in-cell simulations with those derived using a semianalytic model; these results show remarkable agreement, leading to constraints on the axion-photon coupling that typically differ by a factor of no more than ~2. The limits presented here are the strongest to date for axion masses 10^{-8} eV $\lesssim m_a \lesssim 10^{-5}$ eV, and crucially do not rely on the assumption that axions are dark matter.

Introduction.—Axions are among the best-motivated candidates for physics beyond the standard model; these particles are a fundamental prediction of the leading solution to the strong *CP* problem [1–4], are an ideal candidate to explain the "missing matter" in the Universe (i.e., dark matter) [5–8], and are expected to arise naturally in string theory from the compactification of gauge fields on topologically nontrivial manifolds [9,10].

Axions generically couple to electromagnetism via the Lagrangian term $\mathcal{L} = -\frac{1}{4} g_{a\gamma\gamma} \vec{E} \cdot \vec{B} a$, where a is the axion, $\vec{E}$ and $\vec{B}$ are the electric and magnetic fields, and $g_{a\gamma\gamma}$ is a dimensionful coupling constant. This interaction allows for axions and photons to mix in the presence of external magnetic fields, a process which is searched for in both laboratory experiments (e.g., axion haloscopes [11–30], helioscopes [31–33], and light-shining-through-walls experiments [34–36]) and in indirect astrophysical searches, such as those looking for spectral features in x rays and gamma rays (see, e.g., [37–49]) and radio searches for spectral lines [50–52] (note that there also exist searches for radio lines from axion decay [53–57], however the detection prospects are significantly weaker).

One environment in which axion-photon mixing is particularly strong is the magnetosphere of a neutron star, where the large coherent magnetic field and the ambient plasma allow for highly efficient resonant transitions (resonant transitions occur when an axion or photon traverses a medium where the axion and photon momentum are approximately equal, i.e., $k_a \simeq k_\gamma$). If axions contribute to the dark matter, one expects this conversion to generate narrow spectral lines that can be observed using radio telescopes [50–52,58–66]; this idea has ignited numerous observational efforts [50–52], with the most recent study setting world-leading limits for axion masses near ~30 μeV [52]. Despite the success and future promise of these spectral line searches, they are limited by the assumption that axions contribute significantly to dark matter, that the dark matter is smoothly distributed throughout the Galaxy, and that the Galactic dark matter halo is cuspy. Furthermore, such searches are confined to masses 10^{-7} eV $\lesssim m_a \lesssim 10^{-4}$ eV, as the mass must be sufficiently high to produce observable radio emission and sufficiently low so that resonances may be encountered.

Recently, Ref. [67] proposed an alternative way to detect axions in neutron star magnetospheres that overcomes the
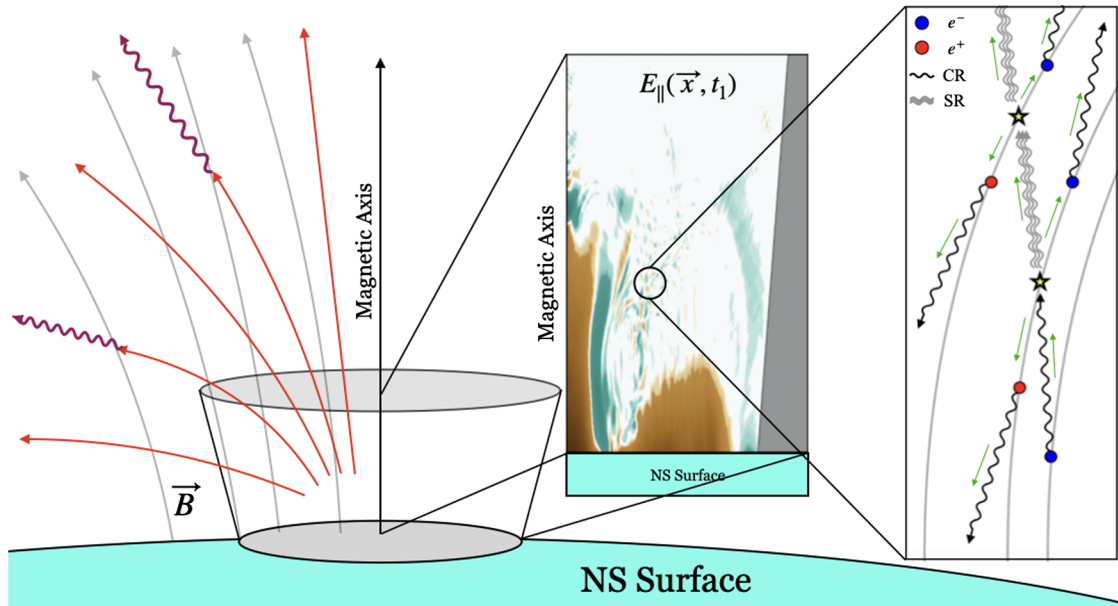
FIG. 1. Schematic figure showing axion production in neutron star vacuum gaps. The vacuum gap is depicted by a truncated cone on the neutron star surface. The left inset shows a time snapshot of $E_\parallel$ (from the simulations of [69]), with the brown and green coloring reflecting negative and positive values of $E_\parallel$. The right inset depicts the microphysical processes responsible for the pair cascade, with green arrows indicating the direction the cascade flows with time. Axions (red) are emitted from the gap and convert to photons (purple) in the presence of the neutron star's magnetic field, $\vec{B}$ (gray).

aforementioned challenges. The idea is based on relativistic axions sourced locally in the magnetosphere from the spacetime oscillations of $\vec{E} \cdot \vec{B}$ (axions may also be produced at the neutron star rotational frequency if there is a large-scale unscreened $\vec{E} \cdot \vec{B}$ [68]). Reference [67] showed that the electromagnetic fields are strong enough in the polar caps of neutron stars [situated above the magnetic poles, and spanning distances of order $r_{\rm pc} \sim \mathcal{O}(10\text{--}100)$ meters—see Fig. 1] to produce an enormous flux of axions. As these axions traverse the magnetosphere they may encounter resonances, generating a broadband radio flux in the MHz–GHz regime. This axion-induced radio flux provides an alternative observable in the search for these evasive particles.

In this Letter, we construct the first pipeline to compute the intrinsic spectrum of axions produced in neutron star polar caps, their resonant conversion to photons, and the nonlinear evolution of these radio photons as they escape the magnetosphere. Our analysis uses both state-of-the-art numerical simulations as well as a newly developed semi-analytic model to predict the axion production rate; the overall agreement of these approaches illustrates that our procedure is not strongly sensitive to reasonable modeling uncertainties in the gap dynamics. We use this pipeline to constrain the axion-photon coupling by comparing the predicted radio flux with measurements of 27 nearby pulsars. The constraints derived here are the strongest to date for axion masses spanning 10^{-8} eV $\lesssim m_a \lesssim 10^{-5}$ eV.

Axion production from vacuum gap discharges.—The $e^\pm$ pair plasma populating the magnetospheres of neutron stars is expected to efficiently screen the component of the background electric field along the magnetic field lines ($E_\parallel$), except in small localized regions referred to as vacuum gaps which are responsible for particle acceleration and production of the pair plasma itself [70,71].

Vacuum gaps are expected to arise in a variety of locations, including in the polar caps [72], the slot gap (located near the neutron star along the last closed field lines) [73], and the outer gap (located near the light cylinder along the last closed field lines) [74]. Recent progress in global particle-in-cell (PIC) simulations of the magnetosphere has shown that $e^\pm$ pairs can be produced in the current sheet near the light cylinder, and efficiently screen gaps situated along the last closed field lines [75,76]. We therefore choose to focus on the dynamics of the vacuum gaps in the polar caps, which also have the highest local values of $\vec{E} \cdot \vec{B}$.

Recently, local PIC simulations of the neutron star polar-cap pair cascade have been performed [69,77,78]. These simulations show that the discharge is an oscillatory process: $e^\pm$ pairs accelerated in the gap produce gamma rays that convert to more $e^\pm$ pairs, which proceed to screen the gap, shutting down pair production [79]. It was proposed that this process can produce coherent electromagnetic radiation, potentially answering the long-standing puzzle of the origin of pulsar radio emission [78].

The oscillatory pair discharge process will in general lead to inductively driven oscillations of $E_\parallel$ at a frequency set by the local plasma frequency, which is expected to evolve from the Goldreich-Julian (GJ) oscillation

frequency $\omega_{\mathrm{GJ}} = \sqrt{4\pi\alpha n_{\mathrm{GJ}}/m_e}$ (we work in units where $c = \hbar = 1$) to a value $\mathcal{O}(10\text{--}100)$ times greater as the density of the pair plasma increases [79–82]. Here we have introduced the GJ charge density, given by $n_{\mathrm{GJ}} \equiv 2\vec{B}_0 \cdot \vec{\Omega}_{\mathrm{NS}}/e$, with B_0 and Ω_{NS} being the surface magnetic field strength and rotational frequency of the neutron star, e the elementary charge, m_e the electron mass, and α the fine structure constant. The presence of an oscillating $E_{\parallel}$ directly enters as a source term in the axion's equation of motion,

$$(\Box + m_a^2)a(x) = -g_{a\gamma\gamma}(\vec{E} \cdot \vec{B})(x). \tag{1}$$

The differential production rate of axions per momenta $\vec{k}$ can subsequently be expressed as [83]

$$\frac{d\dot{N}}{d^3k} = \frac{|\tilde{\jmath}(\vec{k})|^2}{2(2\pi)^3\omega(\vec{k})T}, \tag{2}$$

where $\omega(\vec{k})$ is the axion energy, T is the quasiperiodic timescale of the gap collapse, and $\tilde{\jmath}(\vec{k})$ is the Fourier transform (FT) of the source term,

$$\tilde{\jmath}(\vec{k}) = -g_{a\gamma\gamma} \int d^4x \, e^{ik \cdot x}(\vec{E} \cdot \vec{B})(x). \tag{3}$$

The rate and spectrum of axions produced during the collapse of the vacuum gap is fully determined by the spacetime evolution of $E_{\parallel}$. The condition that axions be on shell inherently connects the spatial and temporal evolution of $E_{\parallel}$, meaning a given k mode can only be produced if the spatial component of the FT contains support on scales $\sim k^{-1}$ *and* the temporal component contains support on scales $\sim(k^2 + m_a^2)^{-1/2}$.

In order to provide a quantitative understanding of axion production, we briefly estimate the production rate for a pulsar with $B_0 = 10^{12}$ G and $\Omega_{\mathrm{NS}} = 2\pi$ Hz. The polar-cap radius for such a pulsar is $r_{\mathrm{pc}} \sim 150$ m, and the maximum value of the unscreened electric field is roughly $E_{\parallel} \sim 6 \times 10^{-6} B_0$, see the Supplemental Material [84]. We expect production to be most efficient when $E_{\parallel}$ is largest, which occurs prior to the screening phase when the characteristic scale is $k_c \sim 2\pi/r_{\mathrm{pc}} \sim 10^{-8}$ eV. Neglecting the phase in Eq. (3), and taking $d^3k/\omega \sim k_c^2$, $T \sim 10^{-7}$ s, and $g_{a\gamma\gamma} \sim 10^{-11}$ GeV^{-1}, we find $\dot{N} \sim \mathcal{O}(10^{50})$ axions per second, which is comparable to the values obtained from more careful calculations in the Supplemental Material [84].

Modeling gap collapse.—We adopt two approaches to estimate the axion spectrum produced from the gap dynamics, one based on a semianalytic model and the other on a numerical simulation.

Semianalytic model: We begin by highlighting the key physical features entering our 2 + 1D semianalytic model;

a more detailed description of each step is deferred to the Supplemental Material [84].

We model two stages of gap evolution: pair cascade and gap collapse. The pair cascade phase begins with an initially unscreened $E_{\parallel}$ and low charge density. As the pair cascade progresses, the number density increases exponentially until it reaches n_{GJ}. At this point the gap locally collapses, marking the end of the pair cascade.

A single seed particle (electron) is assumed to initiate the pair cascade. Because of the presence of $E_{\parallel}$, the electron is accelerated to the radiation-reaction-limited Lorentz factor, γ_{max}, in time t_{acc}. Since particles move along curved field lines, they then emit curvature radiation (CR) photons with characteristic energy $\varepsilon_{\mathrm{CR}} \propto \gamma_{\mathrm{max}}^3/\rho_c$, where ρ_c is the field line curvature [80,109]. CR photons may be absorbed by the magnetic field to produce new pairs and synchrotron photons. Newly produced electrons (positrons) are accelerated away from (towards) the neutron star surface, producing their own CR photons, which may again produce new pairs. Synchrotron photons can also produce new pairs if their mean free path is less than the size of the gap (see Fig. 1).

In our model, we compute the creation positions, times, and energies of all photons and pairs produced by the single seed particle. Our model iterates over "generations" of particles, where the first generation is the seed particle, and generation n particles are sourced by generation $n - 1$. We run five generations of the cascade for different seed particle locations within the gap, identifying points where the plasma density locally reaches n_{GJ} as the starting points for gap collapse—these points, which we refer to as "pair production seeds," define the initial conditions of the semianalytic model (see Supplemental Material [84]).

The initial stages of the gap collapse have been studied using analytic toy models and numerical simulations; in both cases, one expects the initial burst of particle production to induce exponentially damped oscillations in $E_{\parallel}$. These oscillations initially occur locally, and subsequently propagate outwards along the magnetic axis [69,78,82,110–116]. The frequency of the damped oscillations is set by the local plasma frequency (which itself is set by the charge density and typical Lorentz factor), and will evolve from ω_{GJ} (i.e., the minimum value necessary to collapse the gap) to a value 10–100 times greater as more pairs are produced. The characteristic screening timescale t_c is set by the time required for pair production processes to yield a GJ charge density, which is roughly equivalent to the time required to accelerate charges to γ_{max} [82]; for realistic pulsars this timescale lies between 10^{-9}–10^{-6} s.

In order to capture the general features of the gap collapse process, we model the unscreened electric field $E_{\parallel}$ with a static profile, and describe the screening of $E_{\parallel}$ as the combination of outward propagating 2D plane waves. Each plane wave is exponentially damped on a timescale t_c, and has a time-evolving oscillation frequency growing

from an initial value ω_{GJ}. In total, we source four propagating plane waves (this number must be sufficiently large to cover the gap, but cannot be too large as interference effects are not properly accounted for in this treatment; in the Supplemental Material [84] we show that taking 3 or 5 plane waves leads to a negligible difference) evenly spaced across the width of the gap, and with initial conditions determined by the one-dimensional pair-production process discussed above.

PIC simulation: Our second model used to compute the axion spectrum relies on a 2.5 dimensional (2.5D means using azimuthal symmetry to reduce the problem to 2D, but still evolving all 3 components of vector quantities) PIC simulation developed in [81]. Working in axisymmetric cylindrical coordinates (r, z), the authors impose a dipolar magnetic field. A rotating disk of radius r_{pc} is established at the stellar surface to produce a potential drop in the open field line zone of the neutron star. Outside $r = r_{pc}$, $E_\parallel$ is forced to zero to model the plasma-filled closed field line zone. Particles are extracted from the surface at a rate that depends on the local value of $E_\parallel$; these particles are accelerated to the radiation-reaction limit and emit gamma rays through synchrocurvature radiation. Those gamma rays subsequently produce $e^\pm$ pairs in the ultrastrong magnetic field through one-photon magnetic pair production [117]. This process is modeled using the state-of-the-art QED module in the PIC code OSIRIS [118]. Videos showing the dynamical screening of $E_\parallel$ are available at [119]; a snapshot of the simulation is shown in the left inset of Fig. 1.

Performing simulations from first principles of the gap collapse process is extremely challenging due to the large separation of scales between the size of the polar cap and the kinetic scale of the plasma (typically differing by 4–5 orders of magnitude). The simulations performed in [81] overcame this difficulty by rescaling the quantum parameters $\chi_{\pm,\gamma} = \sqrt{(p_\mu F^{\mu\nu})^2}/(B_c m_e)$ for both photon emission and pair production, multiplying them by a numerical constant; here, p_μ is the 4-momentum of the corresponding $e^\pm$ or γ, and $B_c \simeq 4.4 \times 10^3$ G is the Schwinger field strength. This rescaling effectively allows pair production to occur at a much lower voltage drop. However, it also significantly reduces the inherent scale separation in the problem: the kinetic plasma length scale becomes only a few hundredths of the polar-cap size. As a result of this compression of scales, the FT necessarily compresses the power to an artificially narrower range of k modes (the largest scales are expected to be unaffected, however power in small scales, i.e., large k modes, will have been shifted to intermediate scales). We describe in Sec. I of the Supplemental Material [84] a procedure for rescaling the power of the FT, along with additional details on the PIC simulation.

The radio flux.—Once the initial axion spectrum has been determined, we employ an updated version of the ray-tracing algorithm developed in [65] to compute the radio spectrum. We describe the general features of this procedure below, and defer further details to the Supplemental Material [84].

We begin by calculating the rate of axion production for momenta spanning from the escape momentum to $\sim\mathcal{O}(10 \text{ GHz})$ (the phenomenology of gravitationally bound axions differs markedly, and thus we leave a detailed study of bound states to a companion paper [120]). For each momentum state the corresponding axion trajectory is propagated to the light cylinder, and all resonances encountered during propagation are identified. Resonances occur when [65,121]

$$\omega_p^2 \simeq \frac{m_a^2 \omega^2}{m_a^2 \cos^2\theta + \omega^2 \sin^2\theta}, \qquad (4)$$

where θ is the angle between the axion momentum and the magnetic field.

At every level crossing we compute the conversion probability, $P_{a \to \gamma}$, and axion survival probability, $P_{a \to a} = 1 - P_{a \to \gamma}$, and subsequently weight each photon sourced at crossing i by $P_{a \to \gamma}^{(i)} = P_{a \to \gamma} \times \Pi_{j=1}^{i-1} P_{a \to a}^{(j)}$ (we do not compute the axion production probability for subsequent resonances encountered by sourced photons, as this quickly becomes computationally prohibitive; for the pulsars and couplings studied here, we do not expect this secondary contribution to be significant). The conversion probability at an individual level crossing is given by the Landau-Zener formula [62]

$$P_{a \to \gamma} = 1 - e^{-\Gamma}, \qquad (5)$$

with

$$\Gamma = \frac{\pi}{2} \left(1 + \frac{\omega_p^4 \Delta^2 \cos^2\theta}{\omega^4}\right) \left(\frac{\omega g_{a\gamma\gamma} B \Delta}{k_a}\right)^2 \frac{1}{|\partial_s k_\gamma|}. \qquad (6)$$

Here, we have introduced $\Delta \equiv \sin\theta/(1 - \omega_p^2 \cos^2\theta/\omega^2)$ and defined [121]

$$\partial_s \equiv \partial_{\hat{k}_\parallel} - (\omega_p^2 \Delta \cos\theta/\omega^2)\partial_{\hat{k}_\perp}, \qquad (7)$$

with $\hat{k}_\parallel$ ($\hat{k}_\perp$) representing the parallel (perpendicular) direction to the axion momentum. Photons are propagated to the light cylinder using the dispersion relation for a Langmuir-O mode (see Ref. [65]). The observed spectrum is obtained by summing over the final distribution of binned and weighted photons—example spectra are included in the Supplemental Material [84].

Results and discussion.—The radio emission mechanism of active pulsars is not well understood, making it difficult to identify signatures arising from this process. Nevertheless, one can constrain the existence of axions
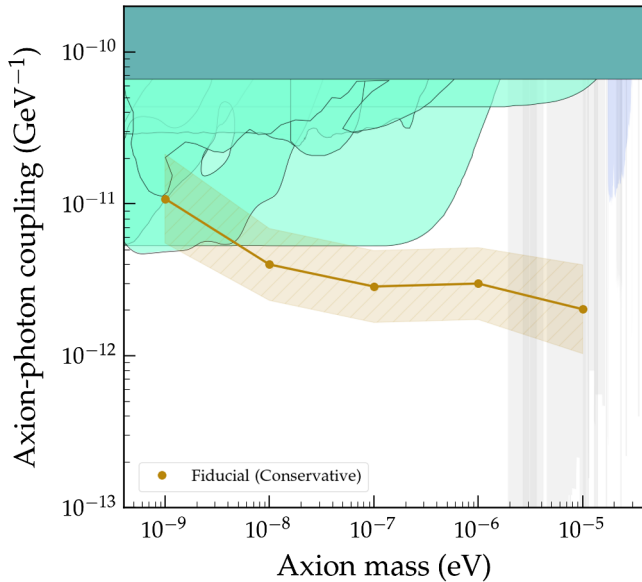
FIG. 2. Upper limits on the axion-photon coupling derived in this Letter using a combination of a 2.5D PIC simulation and the semianalytic model. The band reflects a conservative estimate of the modeling uncertainties (see Supplemental Material [84]). We compare to existing constraints from neutron stars [52] (blue), haloscopes [11–27,122] (gray), helioscopes [33] (teal), and astrophysics [37–46,123,124] (light green). The former two have reduced opacity to highlight that they rely on axions being dark matter.

without knowing the intrinsic pulsar flux by requiring that their contribution not exceed the observed flux. In this section we derive limits on $g_{a\gamma\gamma}$ using observations of 27 nearby pulsars; our sample includes representative nearby pulsars, whose surface magnetic field and rotational period roughly span $10^{12}\,\text{G} \lesssim B_0 \lesssim 10^{13}\,\text{G}$ and $10^{-1}\,\text{s} \lesssim P_{\text{NS}} \lesssim 2\,\text{s}$. For computational ease, we choose to focus on pulsars whose radio emission geometry is constrained by observations, thus evading the need to marginalize over the misalignment and viewing angles. Details of all pulsars used in this analysis are presented in the Supplemental Material [84].

We present our fiducial 95% confidence level upper limits in Fig. 2, which are obtained by computing the constraints for both models (a comparison between models is left to the Supplemental Material [84]) and taking the weaker limit at each mass. The bands around the fiducial limit represent a conservative estimate of the systematic uncertainties (see Supplemental Material [84]). For comparison, we plot constraints from radio line searches using neutron stars (blue), axion haloscopes (grey), the CAST experiment (teal) and x-ray and gamma-ray telescopes (light green). The limits derived in this Letter significantly improve upon existing bounds, and unlike axion haloscope experiments (and radio line searches), do not assume axions contribute to the dark matter. In addition, since the radio flux scales $\propto g_{a\gamma\gamma}^4$, the constraint is largely

insensitive to minor mismodeling errors. The mass range covered by our constraints is limited by the frequency of radio observations (higher frequencies could probe higher masses), and the computational expense (computing time increases at both lower and higher masses).

In the Supplemental Material [84] we show that the derived bound is controlled by observations of a few strong pulsars, with high frequency observations providing the most constraining power. A comprehensive analysis of all pulsars in the ATNF catalog, as well as more dedicated pulsar observations at high frequencies, could significantly improve upon these results; we reserve this broader analysis for future work.

[*]Corresponding author: d.noordhuis@uva.nl
[†]These authors contributed equally to this work.

[1] R. D. Peccei and H. R. Quinn, Phys. Rev. Lett. **38**, 1440 (1977).
[2] R. D. Peccei and H. R. Quinn, Phys. Rev. D **16**, 1791 (1977).
[3] S. Weinberg, Phys. Rev. Lett. **40**, 223 (1978).
[4] F. Wilczek, Phys. Rev. Lett. **40**, 279 (1978).
[5] J. Preskill, M. B. Wise, and F. Wilczek, Phys. Lett. **120B**, 127 (1983).
[6] L. Abbott and P. Sikivie, Phys. Lett. **120B**, 133 (1983).
[7] M. Dine and W. Fischler, Phys. Lett. **120B**, 137 (1983).
[8] N. Aghanim, Y. Akrami, M. Ashdown, J. Aumont, C. Baccigalupi, M. Ballardini, A. Banday, R. Barreiro, N. Bartolo et al. (P. Collaboration), Astron. Astrophys. **641**, A6 (2020).
[9] P. Svrcek and E. Witten, J. High Energy Phys. 06 (2006) 051.
[10] A. Arvanitaki, S. Dimopoulos, S. Dubovsky, N. Kaloper, and J. March-Russell, Phys. Rev. D **81**, 123530 (2010).
[11] P. Sikivie, Phys. Rev. Lett. **51**, 1415 (1983).

[12] S. DePanfilis, A. C. Melissinos, B. E. Moskowitz, J. T. Rogers, Y. K. Semertzidis, W. U. Wuensch, H. J. Halama, A. G. Prodell, W. B. Fowler, and F. A. Nezrick, Phys. Rev. Lett. **59,** 839 (1987).

[13] C. Hagmann, P. Sikivie, N. S. Sullivan, and D. B. Tanner, Phys. Rev. D **42,** 1297 (1990).

[14] C. Hagmann et al. (ADMX Collaboration), Phys. Rev. Lett. **80,** 2043 (1998).

[15] S. J. Asztalos et al. (ADMX Collaboration), Phys. Rev. D **64,** 092003 (2001).

[16] S. J. Asztalos et al. (ADMX Collaboration), Phys. Rev. Lett. **104,** 041301 (2010).

[17] N. Du et al. (ADMX Collaboration), Phys. Rev. Lett. **120,** 151301 (2018).

[18] T. Braine et al. (ADMX Collaboration), Phys. Rev. Lett. **124,** 101303 (2020).

[19] R. Bradley, J. Clarke, D. Kinion, L. J. Rosenberg, K. van Bibber, S. Matsuki, M. Mück, and P. Sikivie, Rev. Mod. Phys. **75,** 777 (2003).

[20] S. J. Asztalos et al., Phys. Rev. D **69,** 011101(R) (2004).

[21] T. M. Shokair et al., Int. J. Mod. Phys. A **29,** 1443004 (2014).

[22] B. M. Brubaker et al. (HAYSTAC Collaboration), Phys. Rev. Lett. **118,** 061302 (2017).

[23] L. Zhong et al. (HAYSTAC Collaboration), Phys. Rev. D **97,** 092001 (2018).

[24] K. M. Backes et al. (HAYSTAC Collaboration), Nature (London) **590,** 238 (2021).

[25] B. T. McAllister, G. Flower, E. N. Ivanov, M. Goryachev, J. Bourhill, and M. E. Tobar, Phys. Dark Universe **18,** 67 (2017).

[26] N. Crescini et al. (QUAX Collaboration), Phys. Rev. Lett. **124,** 171801 (2020).

[27] J. Choi, S. Ahn, B. Ko, S. Lee, and Y. Semertzidis, Nucl. Instrum. Methods Phys. Res., Sect. A **1013,** 165667 (2021).

[28] A. Caldwell, G. Dvali, B. Majorovits, A. Millar, G. Raffelt, J. Redondo, O. Reimann, F. Simon, and F. Steffen (MADMAX Working Group), Phys. Rev. Lett. **118,** 091801 (2017).

[29] B. Majorovits et al. (MADMAX interest Group), J. Phys. Conf. Ser. **1342,** 012098 (2020).

[30] M. Baryakhtar, J. Huang, and R. Lasenby, Phys. Rev. D **98,** 035006 (2018).

[31] E. Arik et al. (CAST Collaboration), J. Cosmol. Astropart. Phys. 02 (2009) 008.

[32] M. Arik et al. (CAST Collaboration), Phys. Rev. D **92,** 021101 (2015).

[33] V. Anastassopoulos et al. (CAST Collaboration), Nat. Phys. **13,** 584 (2017).

[34] K. Van Bibber, N. R. Dagdeviren, S. E. Koonin, A. K. Kerman, and H. N. Nelson, Phys. Rev. Lett. **59,** 759 (1987).

[35] R. Rabadán, A. Ringwald, and K. Sigurdson, Phys. Rev. Lett. **96,** 110407 (2006).

[36] S. L. Adler, J. Gamboa, F. Méndez, and J. López-Sarrión, Ann. Phys. (Amsterdam) **323,** 2851 (2008).

[37] D. Wouters and P. Brun, Astrophys. J. **772,** 44 (2013).

[38] A. Abramowski et al. (H.E.S.S. Collaboration), Phys. Rev. D **88,** 102003 (2013).

[39] A. Payez et al., J. Cosmol. Astropart. Phys. 02 (2015) 006.

[40] M. Ajello et al. (Fermi-LAT Collaboration), Phys. Rev. Lett. **116,** 161101 (2016).

[41] M. Meyer, M. Giannotti, A. Mirizzi, J. Conrad, and M. A. Sánchez-Conde, Phys. Rev. Lett. **118,** 011103 (2017).

[42] M. C. D. Marsh, H. R. Russell, A. C. Fabian, B. P. McNamara, P. Nulsen, and C. S. Reynolds, J. Cosmol. Astropart. Phys. 12 (2017) 036.

[43] C. S. Reynolds, M. C. D. Marsh, H. R. Russell, A. C. Fabian, R. Smith, F. Tombesi, and S. Veilleux, Astrophys. J. **890,** 59 (2020).

[44] M. Xiao, K. M. Perez, M. Giannotti, O. Straniero, A. Mirizzi, B. W. Grefenstette, B. M. Roach, and M. Nynka, Phys. Rev. Lett. **126,** 031101 (2021).

[45] H.-J. Li, J.-G. Guo, X.-J. Bi, S.-J. Lin, and P.-F. Yin, Phys. Rev. D **103,** 083003 (2021).

[46] C. Dessert, J. W. Foster, and B. R. Safdi, Phys. Rev. Lett. **125,** 261102 (2020).

[47] M. Meyer and T. Petrushevska, Phys. Rev. Lett. **124,** 231101 (2020); **125,** 119901(E) (2020).

[48] F. Calore, P. Carenza, C. Eckner, T. Fischer, M. Giannotti, J. Jaeckel, K. Kotake, T. Kuroda, A. Mirizzi, and F. Sivo, Phys. Rev. D **105,** 063028 (2022).

[49] J. S. Reynés, J. H. Matthews, C. S. Reynolds, H. R. Russell, R. N. Smith, and M. C. D. Marsh, Mon. Not. R. Astron. Soc. **510,** 1264 (2021).

[50] J. W. Foster, Y. Kahn, O. Macias, Z. Sun, R. P. Eatough, V. I. Kondratiev, W. M. Peters, C. Weniger, and B. R. Safdi, Phys. Rev. Lett. **125,** 171301 (2020).

[51] R. A. Battye, J. Darling, J. McDonald, and S. Srinivasan, Phys. Rev. D **105,** L021305 (2022).

[52] J. W. Foster, S. J. Witte, M. Lawson, T. Linden, V. Gajjar, C. Weniger, and B. R. Safdi, Phys. Rev. Lett. **129,** 251102 (2022).

[53] A. Caputo, C. P. n. Garay, and S. J. Witte, Phys. Rev. D **98,** 083024 (2018); **99,** 089901(E) (2019).

[54] A. Caputo, M. Regis, M. Taoso, and S. J. Witte, J. Cosmol. Astropart. Phys. 03 (2019) 027.

[55] O. Ghosh, J. Salvado, and J. Miralda-Escudé, arXiv:2008.02729.

[56] M. A. Buen-Abad, J. J. Fan, and C. Sun, Phys. Rev. D **105,** 075006 (2022).

[57] Y. Sun, K. Schutz, A. Nambrath, C. Leung, and K. Masui, Phys. Rev. D **105,** 063007 (2022).

[58] M. S. Pshirkov and S. B. Popov, J. Exp. Theor. Phys. **108,** 384 (2009).

[59] F. P. Huang, K. Kadota, T. Sekiguchi, and H. Tashiro, Phys. Rev. D **97,** 123001 (2018).

[60] A. Hook, Y. Kahn, B. R. Safdi, and Z. Sun, Phys. Rev. Lett. **121,** 241102 (2018).

[61] B. R. Safdi, Z. Sun, and A. Y. Chen, Phys. Rev. D **99,** 123021 (2019).

[62] R. A. Battye, B. Garbrecht, J. I. McDonald, F. Pace, and S. Srinivasan, Phys. Rev. D **102,** 023504 (2020).

[63] M. Leroy, M. Chianese, T. D. P. Edwards, and C. Weniger, Phys. Rev. D **101,** 123003 (2020).

[64] J. H. Buckley, P. B. Dev, F. Ferrer, and F. P. Huang, Phys. Rev. D **103,** 043015 (2021).

[65] S. J. Witte, D. Noordhuis, T. D. P. Edwards, and C. Weniger, Phys. Rev. D **104,** 103030 (2021).

[66] R. A. Battye, B. Garbrecht, J. McDonald, and S. Srinivasan, J. High Energy Phys. 09 (2021) 105.

[67] A. Prabhu, Phys. Rev. D **104**, 055038 (2021).

[68] B. Garbrecht and J. I. McDonald, J. Cosmol. Astropart. Phys. 07 (2018) 044.

[69] F. Cruz, T. Grismayer, A. Y. Chen, A. Spitkovsky, and L. O. Silva, Astrophys. J. Lett. **919**, L4 (2021).

[70] P. Goldreich and W. H. Julian, Astrophys. J. **157**, 869 (1969).

[71] J. Chiang and R. W. Romani, Astrophys. J. **400**, 629 (1992).

[72] M. A. Ruderman and P. G. Sutherland, Astrophys. J. **196**, 51 (1975).

[73] J. Arons, Astrophys. J. **266**, 215 (1983).

[74] K. S. Cheng, C. Ho, and M. Ruderman, Astrophys. J. **300**, 500 (1986).

[75] G. Brambilla, C. Kalapotharakos, A. N. Timokhin, A. K. Harding, and D. Kazanas, Astrophys. J. **858**, 81 (2018).

[76] R. Hu and A. M. Beloborodov, Astrophys. J. **939**, 42 (2022).

[77] A. N. Timokhin and J. Arons, Mon. Not. R. Astron. Soc. **429**, 20 (2013).

[78] A. Philippov, A. Timokhin, and A. Spitkovsky, Phys. Rev. Lett. **124**, 245101 (2020).

[79] A. Levinson, D. Melrose, A. Judge, and Q. Luo, Astrophys. J. **631**, 456 (2005).

[80] A. N. Timokhin and A. K. Harding, Astrophys. J. **810**, 144 (2015).

[81] F. Cruz, T. Grismayer, and L. O. Silva, Astrophys. J. **908**, 149 (2021).

[82] E. A. Tolman, A. A. Philippov, and A. N. Timokhin, Astrophys. J. Lett. **933**, L37 (2022).

[83] M. E. Peskin, *An Introduction to Quantum Field Theory* (CRC Press, Boca Raton, 2018).

[84] See Supplemental Material at http://link.aps.org/supplemental/10.1103/PhysRevLett.131.111004 for further discussion pertaining to vacuum gap modeling, which includes Refs. [85,86]; radio flux computation, which includes Ref. [87]; properties of used pulsars, which includes Refs. [88–98]; our profile likelihood analysis, which includes Refs. [99–101]; and uncertainties, which includes Refs. [102–108].

[85] R. Fonseca, S. Martins, L. Silva, J. Tonge, F. Tsung, and W. Mori, Plasma Phys. Controlled Fusion **50**, 124034 (2008).

[86] A. N. Timokhin and A. K. Harding, Astrophys. J. **871**, 12 (2019).

[87] P. Carenza and M. C. D. Marsh, J. Cosmol. Astropart. Phys. 04 (2023) 021.

[88] L. Bondonneau, J.-M. Grießmeier, G. Theureau, A. Bilous, V. Kondratiev, M. Serylak, M. Keith, and A. Lyne, Astron. Astrophys. **635**, A76 (2020).

[89] D. Lorimer, J. Yates, A. Lyne, and D. Gould, Mon. Not. R. Astron. Soc. **273**, 411 (1995).

[90] R.-S. Zhao *et al.*, Astrophys. J. **845**, 156 (2017).

[91] J. M. Rankin, Astrophys. J. **405**, 285 (1993).

[92] Y. Gupta and R. Gangadhara, Astrophys. J. **584**, 418 (2003).

[93] J. Rankin, Mon. Not. R. Astron. Soc. **514**, 3202 (2022).

[94] J. P. W. Verbiest, J. M. Weisberg, A. A. Chael, K. J. Lee, and D. R. Lorimer, Astrophys. J. **755**, 39 (2012).

[95] J. Yao, R. Manchester, and N. Wang, Astrophys. J. **835**, 29 (2017).

[96] S. Brownsberger and R. W. Romani, Astrophys. J. **784**, 154 (2014).

[97] D. C. Price, C. Flynn, and A. Deller, Pub. Astron. Soc. Aust. **38**, e038 (2021).

[98] F. Jankowski, W. van Straten, E. F. Keane, M. Bailes, E. D. Barr, S. Johnston, and M. Kerr, Mon. Not. R. Astron. Soc. **473**, 4436 (2018).

[99] S. S. Wilks, Ann. Math. Stat. **9**, 60 (1938).

[100] A. Wald, Trans. Am. Math. Soc. **54**, 426 (1943).

[101] G. Cowan, K. Cranmer, E. Gross, and O. Vitells, Eur. Phys. J. C **71**, 1554 (2011); **73**, 2501(E) (2013).

[102] J. Li, A. Spitkovsky, and A. Tchekhovskoy, Astrophys. J. Lett. **746**, L24 (2012).

[103] A. W. Steiner, S. Gandolfi, F. J. Fattoyev, and W. G. Newton, Phys. Rev. C **91**, 015804 (2015).

[104] J. M. Lattimer, Annu. Rev. Nucl. Part. Sci. **71**, 433 (2021).

[105] V. Radhakrishnan and D. Cooke, Astrophys. Lett. **3** 225 (1969).

[106] A. M. Beloborodov, Astrophys. J. **683**, L41 (2008).

[107] M. A. Belyaev and K. Parfrey, Astrophys. J. **830**, 119 (2016).

[108] A. Szary, G. I. Melikidze, and J. Gil, Mon. Not. R. Astron. Soc. **447**, 2295 (2015).

[109] J. D. Jackson, *Classical Electrodynamics* (Wiley, New York, 1998).

[110] A. Levinson, D. Melrose, A. Judge, and Q.-h. Luo, Astrophys. J. **631**, 456 (2005).

[111] A. N. Timokhin, Mon. Not. R. Astron. Soc. **408**, 2092 (2010).

[112] A. Levinson and B. Cerutti, Astron. Astrophys. **616**, A184 (2018).

[113] A. Y. Chen and Y. Yuan, Astrophys. J. **895**, 121 (2020).

[114] S. Kisaka, A. Levinson, and K. Toma, Astrophys. J. **902**, 80 (2020).

[115] F. Cruz, T. Grismayer, and L. O. Silva, Astrophys. J. **908**, 149 (2021).

[116] F. Cruz, T. Grismayer, S. Iteanu, P. Tortone, and L. O. Silva, Phys. Plasmas **29**, 052902 (2022).

[117] T. Erber, Rev. Mod. Phys. **38**, 626 (1966).

[118] R. A. Fonseca, L. O. Silva, F. S. Tsung, V. K. Decyk, W. Lu, C. Ren, W. B. Mori, S. Deng, S. Lee, T. Katsouleas *et al.*, in *Proceedings of the International Conference on Computational Science* (Springer, New York, 2002), pp. 342–351.

[119] https://www.youtube.com/watch?v=wHSw5kp7Ik4online.

[120] D. Noordhuis, A. Prabhu, C. Weniger, and S. J. Witte, arXiv:2307.11811v1.

[121] A. J. Millar, S. Baum, M. Lawson, and M. C. D. Marsh, J. Cosmol. Astropart. Phys. 11 (2021) 013.

[122] A. Álvarez-Melcón *et al.*, J. High Energy Phys. 10 (2021) 075.

[123] C. Dessert, A. J. Long, and B. R. Safdi, Phys. Rev. Lett. **128**, 071102 (2022).

[124] C. Dessert, D. Dunsky, and B. R. Safdi, Phys. Rev. D **105**, 103034 (2022).

[125] C. O'Hare, cajohare/axionlimits: Axionlimits, 10.5281/zenodo.3932430 (2020).